JVST B
Journal of Vacuum Science & Technology B

Study of a linear surface wave plasma source for tin removal in an extreme ultraviolet source

Cite as: J. Vac. Sci. Technol. B **38**, 052601 (2020); https://doi.org/10.1116/6.0000200
Submitted: 20 July 2020 . Accepted: 03 August 2020 . Published Online: 21 August 2020

Dren Qerimi, Gianluca Panici, Arihant Jain, Daniel Jacobson, David N. Ruzic, et al.

View Online

Export Citation

CrossMark

ARTICLES YOU MAY BE INTERESTED IN

In situ collector cleaning and extreme ultraviolet reflectivity restoration by hydrogen plasma for extreme ultraviolet sources
Journal of Vacuum Science & Technology A **34**, 021305 (2016); https://doi.org/10.1116/1.4942456

Determination of recombination coefficients for hydrogen, oxygen, and nitrogen gasses via in situ radical probe system
Journal of Vacuum Science & Technology A **39**, 023004 (2021); https://doi.org/10.1116/6.0000787

Radical probe system for in situ measurements of radical densities of hydrogen, oxygen, and nitrogen
Journal of Vacuum Science & Technology A **39**, 023003 (2021); https://doi.org/10.1116/6.0000786

Advance your science and career as a member of AVS

LEARN MORE

© 2020 Author(s).

JVST B
Journal of Vacuum Science & Technology B

ARTICLE

avs.scitation.org/journal/jvb

Study of a linear surface wave plasma source for tin removal in an extreme ultraviolet source

Cite as: J. Vac. Sci. Technol. B **38**, 052601 (2020); doi: 10.1116/6.0000200
Submitted: 20 July 2020 · Accepted: 3 August 2020 ·
Published Online: 21 August 2020

View Online

Export Citation

CrossMark

Dren Qerimi, Gianluca Panici, Arihant Jain, Daniel Jacobson, and David N. Ruzic[a)]

AFFILIATIONS

Department of Nuclear, Plasma, and Radiological Engineering, Center for Plasma-Material Interactions, University of Illinois at Urbana-Champaign, 216 Talbot Lab, 104 S. Wright St., Urbana, Illinois 61801

[a)]**Electronic mail:** druzic@illinois.edu

ABSTRACT

Tin deposition mitigation employs hydrogen radicals and ions, formed in a hydrogen plasma, to interact with tin to form tin hydride (SnH_4) in the gaseous state, which is then pumped away. Surface wave plasma (SWP) technology developed at Illinois generates hydrogen radicals and ions, resulting in tin etch rates that are high enough to keep extreme ultraviolet (EUV) lithographic tools clean. An advantage of an SWP antenna is the ability to generate a high density of hydrogen radicals and hydrogen ions directly at the desired etching location. *In situ* etching of tin enables high availability EUV tools by maintaining high reflectivity of the multilayer mirror of the collector. Additionally, the SWP is characterized with low ion energies and low electron temperature, such that the multilayer mirror does not suffer any damage from sputtering or implantation of hydrogen ions during operation. Here, experiments elucidating the fundamental processes of tin removal are conducted by varying pressure, power, surface temperature, and gas flow rate in order to observe the etch rate behavior. Our results have shown that the presence of hydrogen ions increases etch rates because ion bombardment weakens Sn–Sn bonds, which, in turn, allows for a higher rate of chemical etching by the radicals. The ion bombardment reduces the number of radicals needed to etch a single tin atom to the range of 10^2–10^3. The linear SWP antenna yields plasma densities on the order of 10^{17} to 10^{18} m^{-3} and radical densities on the order of 10^{18} to 10^{19} m^{-3}, allowing for greater utilization of ion etch enhancement. Etch rates of up to 200 nm/min have been achieved. The surface temperature of the samples is an important factor in the etching process such that the decrease in the surface temperature increases the etch rates and decreases the hydrogen desorption rates. In addition, a kinetic etch model is developed to explain the behavior of etch rates as a function of surface temperature. Furthermore, results from experiments performed in an Illinois NXE:3100 chamber will be discussed.

Published under license by AVS. https://doi.org/10.1116/6.0000200

I. INTRODUCTION

Extreme ultraviolet (EUV) lithography tools are the leading technologies responsible for the next generation of chip manufacturing. EUV has shown to accurately and precisely pattern wafers but still lags in the wafer production rate compared to previous high-volume manufacturing. Source availability is a key issue to be addressed in order to achieve a higher speed.[1] In an EUV source, a plasma is generated when a CO_2 pulsed laser hits molten droplets of tin, and it ionizes tin in the +8 to +12 range, which then emit 13.5 nm photons. A multilayer mirror (MLM) collector reflects the light toward a series of optic mirrors until EUV lights reaches the wafer.[2] During de-excitation of the Sn plasma, droplets and atoms of Sn deposit on the inner surfaces of the source, including the walls and the collector mirror. Sn film deposits absorb 13.5 nm photons, reducing the reflectivity that leads to severe drop in source power at the wafer. Conventional Sn cleaning is a multiday process, thus causing major downtime for the tool. An *in situ* tin etch method increases lifetimes of the EUV source including collector and plasma facing components. One advantage of using hydrogen gas inside an EUV source is that hydrogen radicals are produced and chemically etch Sn away to form tin hydride.[3] Having shown previously the ability of tin etching in hydrogen plasmas[4] and recovery of near total reflectivity,[5] this study shows Sn removal from any surface in an EUV source as a function of surface temperature. Also, previous work has shown that the highest etch rates occur when plasma is in the reactive ion etch regime.[4,5] A linear surface wave plasma (SWP) is used replicating actual source conditions (pressure, gas flow rate, and geometry) in the Illinois NXE:3100 system. SWP

Published under license by AVS.

has high hydrogen radical and ion densities, while electron and ion energies are low in order to avoid damage to the MLM. Very high etch rates have been observed, up to 200 nm/min with ion and radical densities on the order of 10^{12} to 10^{13} cm^{-3} and 10^{14} cm^{-3}, respectively. A custom launcher and an antenna structure were built to interface with the present source geometry. Similar SWP sources were brought to ASML San Diego in order to gauge effectiveness and then tested at the Illinois NXE:3100 system. Results from these experiments are presented in this paper.

II. EXPERIMENT

A series of tests were conducted in an NXE:3100 source at Illinois, where a 28 cm custom machined antenna linear SWP is installed inside the chamber such that conditions of an actual source are replicated: geometry, hydrogen flow rate, pressure, and pumping speed. The linear SWP source is a simple design where an inner conducting rod cased by alumina as a dielectric material is then covered by a ground shield, see Fig. 1. A Kovar ring serves as a bridge between the ground shielding and alumina. A hermetic seal between alumina and the Kovar alloy ring is achieved by brazing via a silver plate and the seal between the ground shielding and the Kovar alloy ring is achieved via laser welding. The gap between the conducting rod and alumina is at atmospheric pressure. However, SWP sources can be designed in various geometrical forms, see patent.[6] Outside the Illinois NXE:3100 source, the linear SWP antenna is connected to a microwave power supply, via a stub tuner acting as a matching network, capable of generating 120 W as maximum output power.

The linear SWP source is placed inside the Illinois NXE:3100 source chamber in a vertical position such that the hydrogen gas flow hits it directly from the center of the collector mirror, see Fig. 2. A linear motion feedthrough from the top of the chamber controls the movement of the radical probe system that measures *in situ* hydrogen radical density by scanning alongside the length of the antenna during each test. The radical probe system based on the work by Mozetič *et al.*[8] has been developed by the Center for Plasma and Material Interactions (CPMI), see MS thesis on the topic.[9] Upcoming

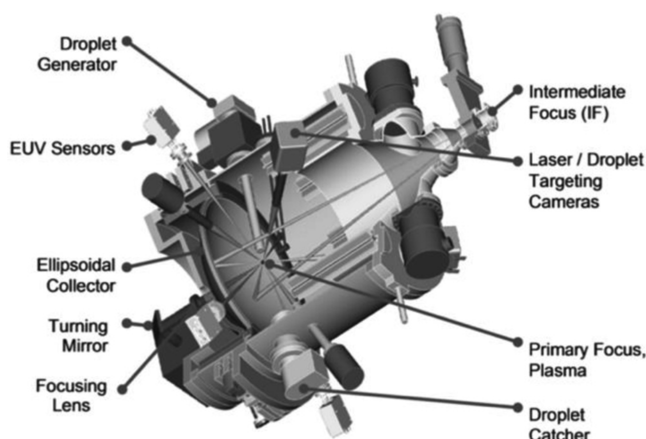

FIG. 2. NXE:3100 detailed schematics showing metrology tools, droplet generator, laser, and plasma formation in the tool source as described in Ref. 7.

papers show how the recombination coefficient is determined by comparing known models with experimental measurements, which, in turn, produces an absolute radical density value.

Additionally, in the same line of sight with radical probes is a Langmuir probe, which is used to diagnose plasma parameters: ion density and electron temperature. Data were collected along the 28 cm length of the SWP antenna with the Langmuir and radical probes at each position. Silicon samples are coated with 1–2 μm of tin film in a separate chamber via argon plasma magnetron sputtering; samples are processed right before each etch test in order to minimize contamination and air exposure. Tin coated samples are placed in a vertical mounted sample holder and placed less then 1 cm from the linear SWP source as shown in Fig. 3. Samples are half masked by a bare silicon sample and kept at a set temperature via a cooling pate attached in the back of the sample holder through thermal paste. After each test, the etched profile thickness is determined by a laser 3D optical profilometer and by a

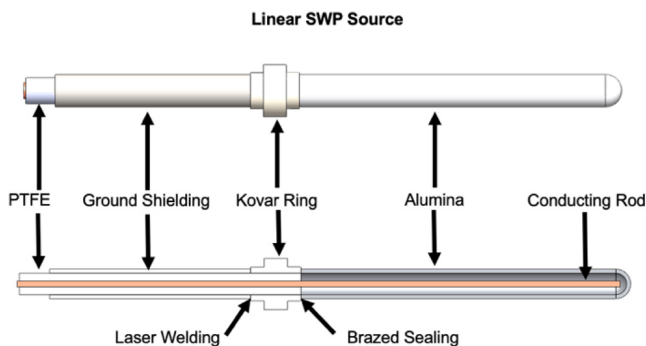

FIG. 1. Linear SWP antenna schematics; a hermetic seal is the SWP source in Illinois achieved by laser welding copper with Kovar and brazed sealing of alumina and Kovar.

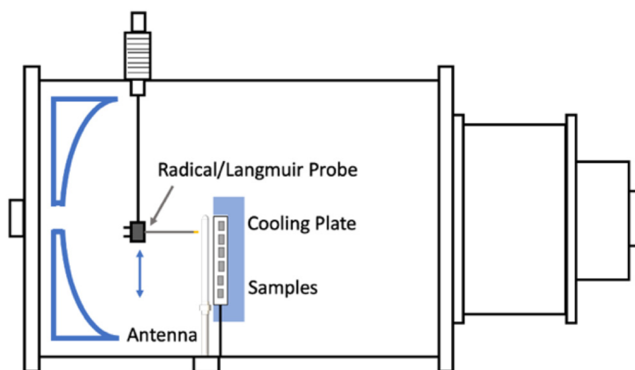

FIG. 3. Vertical sample holder with mounted Sn samples in the Illinois NXE 3100 chamber.

Published under license by AVS.

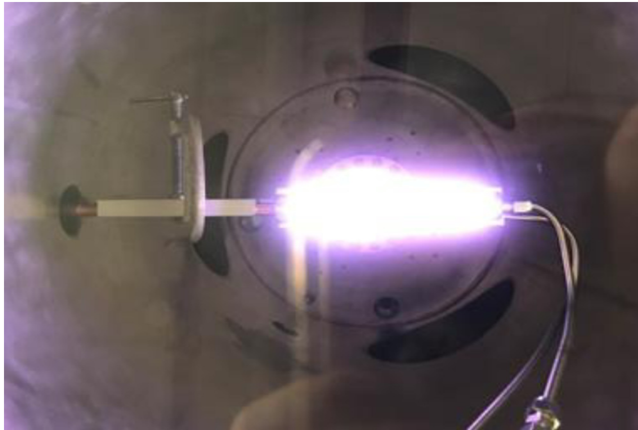

FIG. 4. Operating linear SWP source in Illinois NXE:3100 with a pressure of 1.5 T, a power of 80 W, and a hydrogen flow rate of 100 SLM.

conventional stylus based profilometer. Usually, tests were conducted over a period of time of less than 10 min. Parameters such as varying power, pressure, hydrogen flow, and sample temperature were tested with respect to the tin etch rate. Figure 4 shows plasma coverage of linear SWP while operating at a pressure of 1 Torr, a power of 80 W, and a hydrogen flowrate of 70 SLM.

III. RESULTS AND DISCUSSION

Several tests were carried out in the Illinois NXE:3100 EUV source in order to determine conditions for high etch rates and to diagnose plasma parameters such as hydrogen electron, ion, and radical density by varying pressure, power, flowrate, and temperature. Hydrogen radical densities were measured along the linear SWP source, and it was observed that radical densities varied minimally; therefore, an average radical density is calculated for each test configuration despite the fact that seven measurements were collected along the 28 cm linear SWP antenna. Figure 5 shows average radical densities with respect to power, flowrate, and pressure. To remove tin from the surface, four hydrogen radicals are needed to tin hydride. The competing reaction is that two hydrogen radicals form H_2 and desorb. Experimental parameters of 100 SLM of hydrogen flowrate and 1.5 Torr of pressure are the actual parameters in running an NXE tool. Figure 5(a) shows the behavior of radical density with the increase in power, such that even a non-significant increase of 20W yields higher radical density. It is also observed that with the increasing flowrate, radical density is decreased via enhanced particle transport due to the higher flowrate as shown in Fig. 5(b). However, with varying pressure, the radical density change is not significant due to the nature of surface wave plasma, which travels along the surface and not in the volume, see Fig. 5(c). Mozetic *et al.* have shown similar results[10] with regard to pressure variation. As expected, higher microwave power will break more hydrogen bonds and, thus, generate higher radical densities.

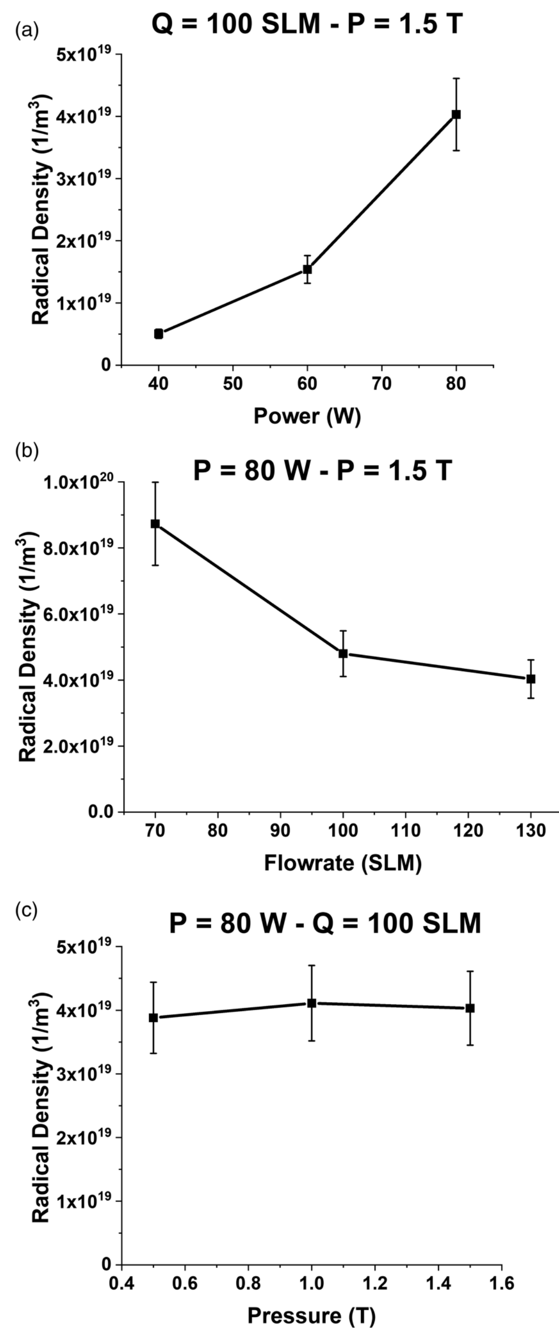

FIG. 5. Averaged measurements of hydrogen radical densities along the length of the linear EUV source with varying power (a), flowrate (b), and pressure (c).

Simultaneously with the radical probe, a Langmuir probe is used to collect data at the same points along the antenna under the same experimental setup and parameters. Three subfigures of ion density radial measurements are shown under same experimental

Published under license by AVS.

parameters. It is observed that ion density increases with power and decreases with pressure, see Figs. 6(a) and 6(c). Maximum ion density with respect to flowrate occurs at 100 SLM. Generally, there are brighter plasma nodes at 2 and 27 cm along this antenna.

As with the case of radical densities, ion density radial measurements are averaged and plotted together with electron temperature in Fig. 7. SWP is characterized with low electron temperature that is essential because a low electron temperature means a small sheath drop and does not impact the collector in terms of damaging multilayers and thus compromising reflectivity. As expected, the electron temperature increases as pressure decreases due to the increased mean free path inside the chamber which reduces the number of collisions, see Fig. 7(c). Ion density decreases as well with the increase in pressure because less plasma is created, and the surface area of the plasma converge shrinks. The flowrate seems to have only a small correlation with ion density and electron temperature. Similarly, to radical densities, higher power generates higher electron temperature and ion density because higher microwave power enables interactions with higher momentum exchange. High ion density is essential to tin etching because incident ions weaken Sn–Sn bonds on the surface. Figure 7 shows the relationship of ion density and electron temperature with respect to power, flowrate, and pressure.

Finally, etch rates were determined with respect to varying parameters including sample temperature. Previously, temperature was not taken into account because the sample temperature on a cooled sample holder does not necessarily affect plasma parameters. However, it is worth to note that radical and Langmuir probes are equidistant with samples from the antenna. Power radiation of the linear SWP source is equal in all directions along the outer perimeter. Previous studies have shown that higher power always yields higher etch rates. The whole goal of this work is to achieve an etch rate that is higher than the source contamination rate in order to decrease down time and increase availability of an NXE tool. Flow dependence is most noticeable nearest to plasma nodes, but the key is that etching occurs at a high rate even at relatively high flowrates. Etch rates as shown in the graphs below, see Fig. 8, where sample No. 1 is near the 2 cm node and sample No. 5 is at 20 cm, which is far away from the node, are up to 200 nm/min that far exceeds the expected contamination rate of the source. Etch rates are exceptionally high for relatively low RF power, implying that an NXE source could remain contamination free at all times with minimal additional energy consumption. Etch rate decreases for samples further away, as can be seen in Fig. 8. Figure 8(b) shows a behavior such that lower hydrogen pressure yields higher etch rate; however, the difference in the flow rate does not translate in the difference in the etch rate further away from the node. In Fig. 8(c), temperatures are at a fixed coolant flow rate from cooling the sample holder maintaining constant temperature during the etch process. Lower temperatures increase the etch rate even at the furthest node. Overall, these results show exceptionally high etch rates compared to surface contamination rates.

An important factor in an etching process is the number of hydrogen radicals needed to etch a single tin atom. The etching reaction is exothermic and proceeds spontaneously,[11]

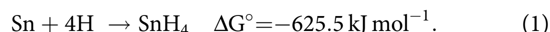

$$Sn + 4H \rightarrow SnH_4 \quad \Delta G^{\circ} = -625.5\,\text{kJ mol}^{-1}. \tag{1}$$

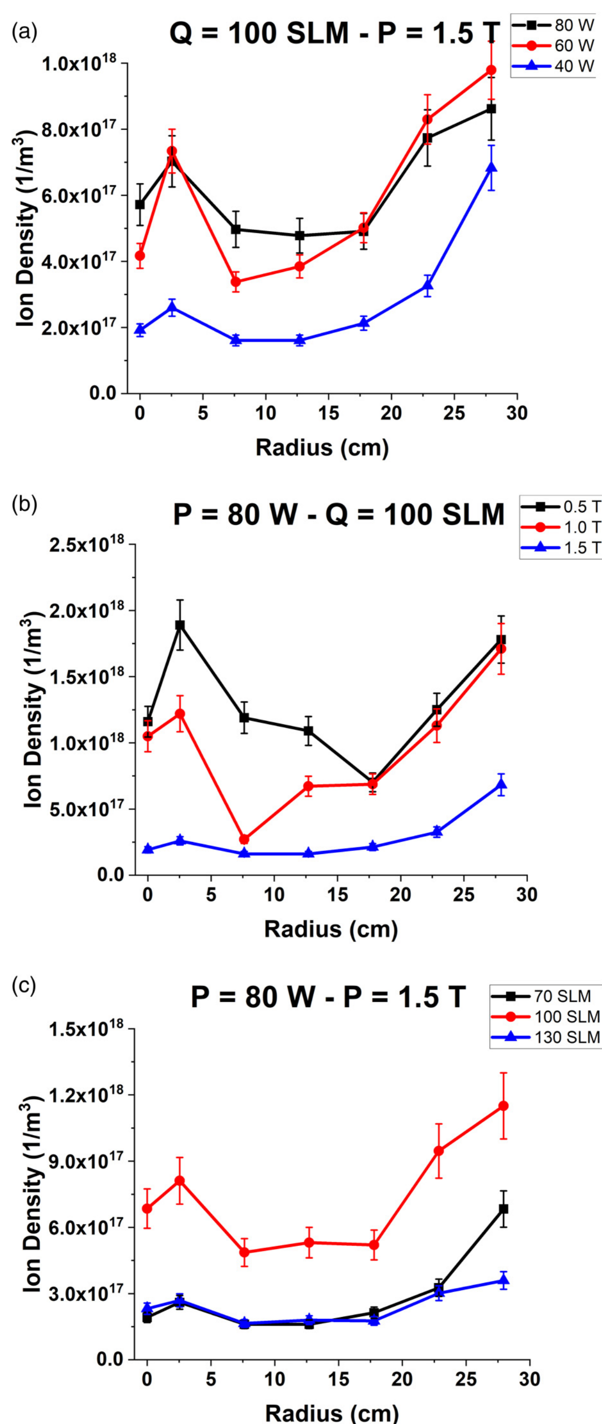

FIG. 6. Radial measurements of hydrogen ion densities with respect to microwave power (a), hydrogen pressure (b), and flowrate (c). This is a sample measurement of a radial scan along the length of the linear SWP source (zero radius is at the bottom of the probe and r = 28 cm is at the antenna tip), which is represented as in Fig. 2.

Published under license by AVS.

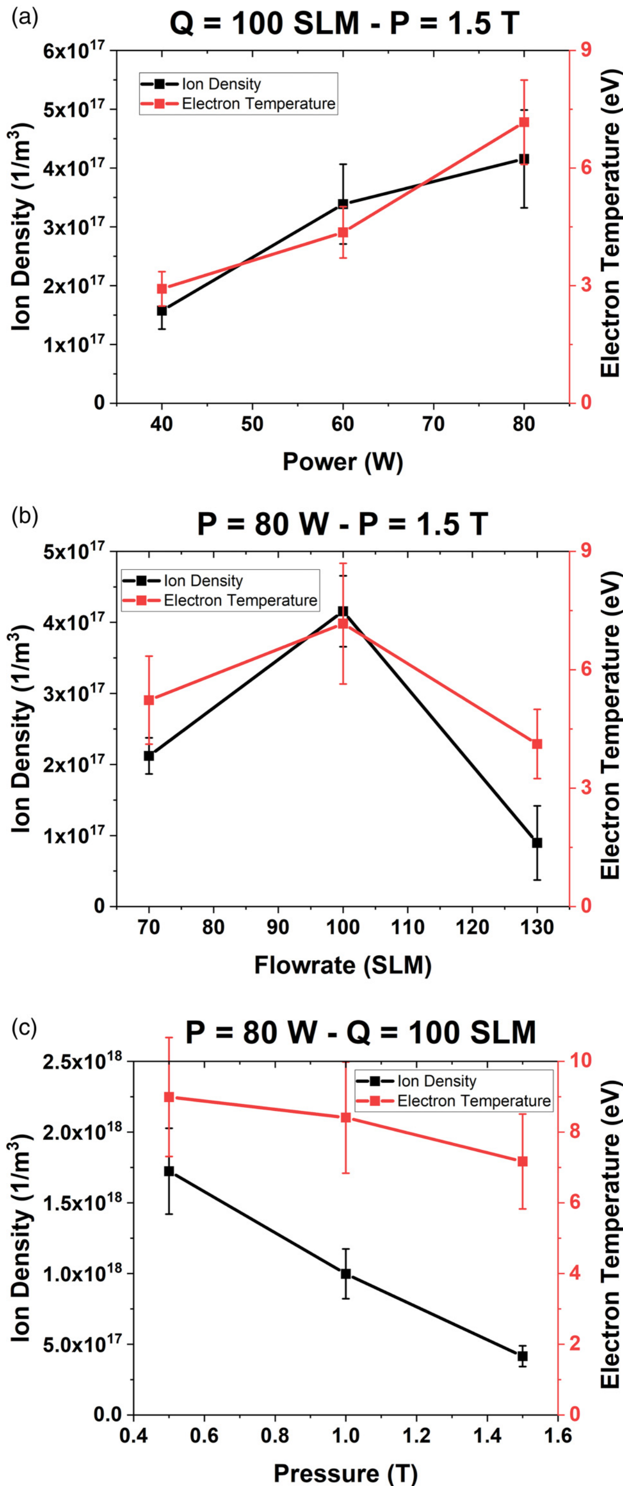

FIG. 7. Relationship of electron temperature and electron density with microwave power (a), hydrogen flowrate (b), and pressure (c).

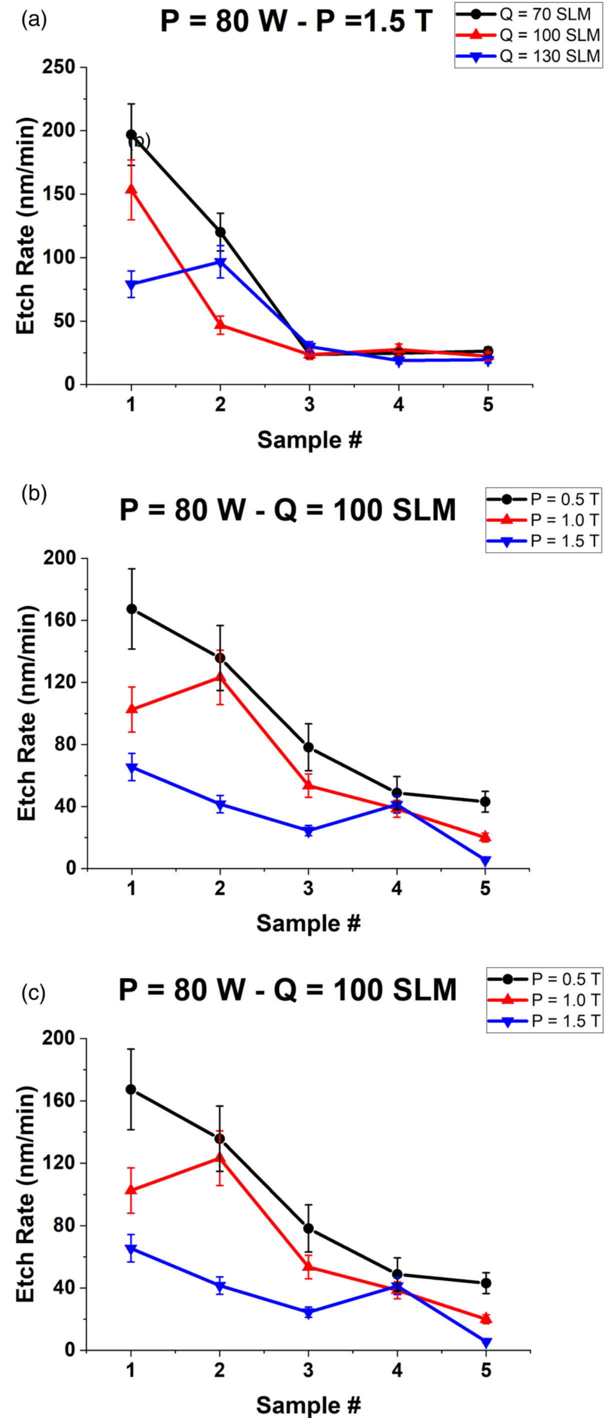

FIG. 8. Tin etch rate measurements at the Illinois NXE:3100 source with respect to flowrate (a), pressure (b), and temperature (c). It is important to note that the sample placement is with respect to node formation from the RF waves. Sample 1 is at the node near the tip of the linear SWP source (2 cm), and the sample is around 20 cm, with the others spaced in between.

Published under license by AVS.

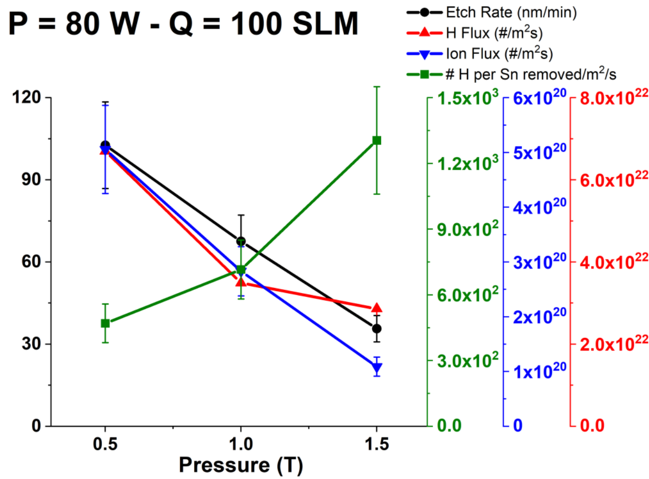

FIG. 9. Dependence of the etch rate with the H radical flux, the ion flux, and the number of H radicals need per tin etch. With the presence of ions, the number of H radicals per Sn removed /m²/s ranges between 10^2 and 10^3.

Every SnH_4 generated during an etch process follows from Eq. (1); thus, four hydrogen radicals are needed to etch a tin atom. However, hydrogen radicals are more thermodynamically favored to recombine with each other than to etch since $\Delta G^\circ = -203.3$ kJ mol^{-1} per one H recombination reaction where only two atoms need to find one another, compared to $\Delta G^\circ = -625.5$ kJ mol^{-1} for etching,[12] but where four atoms have to find the same Sn site. Therefore, most of the H radicals will recombine and in order to determine the actual number of hydrogen radical present needed to etch, the hydrogen surface coverage needs to be calculated. To determine that coverage, we start with

$$\Gamma_{H^*} = \frac{1}{4} n_{H^*} v_{TH}(H^*), \tag{2}$$

$$\Gamma_{SnH_4} = \text{Etch rate}^* N_{Sn}, \tag{3}$$

where $v_{TH}(H^*)$ is thermal velocity of H radicals, n_H^* is H radical density, and $N_{Sn} = \rho_{Sn}{}^* N_{Av}/molar\ mass$ is number density. By dividing Eqs. (2) and (3), the number of H radicals need to be present in order to etch a tin atom range between 10^2 and 10^3. This efficiency is achieved due to high density ions. Without the presence of ions in the etching process, the number increases to between 10^4 and 10^5 radicals.[12,13] Figure 9 shows the relationship between the etch rate, the H radical flux, the hydrogen ion flux, and the number of H radicals/Sn with pressure. It is observed that as the fluxes decrease the number of radical needs per tin atom etch increases. As shown by Elg *et al.*[14] and Rossen and Sawin,[15] ion-enhanced etching increases etch rates because incident ions break the bonds between molecules, thus allowing for easier etch process to be followed by hydrogen radicals. Table I shows the important dependence of the etch rate and the number of H radicals per Sn atom etched with respect to the sample temperature despite the fact that experimental plasma parameters do not change, namely, P = 80 W, P = 1.5 T, and Q = 100 SLM of hydrogen, which implies that the H radical and the ion flux do not change, but the sample temperature itself acts as a driving factor that reduces the number of H radicals/Sn atom as the temperature decreases yielding higher etch rate. Equation (6) represents the relationship between the etch rate and the temperature based on Eq. (3) according to Lieberman and Lichtenberg[16] and Gerlach-Mayer.[17] To calculate it, let θ be the fraction of surface sites covered by H, $K_{ads} = s(T)\sqrt{8k_B T_H/\pi m_H}/4n'$ is the hydrogen radical adsorption rate coefficient and s is the sticking coefficient, $s(T) \approx 1/(1+\exp(776/T(K)))$.[18] $K_{des} = K_0 e^{-\frac{\epsilon_{des}}{T}}$ is the stannane and hydrogen desorption rate equation, where T is the surface temperature, with $K_0(H_2) \approx 1.5{*}10^9\ s^{-1}$ and $K_0(SnH_4) \approx 10^8\ s^{-1}$, respectively, and $\epsilon_{des}(H_2) \approx 0.46$ eV and $\epsilon_{des}(SnH_4) \approx 0.54$ eV, respectively.[19–21] Regarding the desorption rate coefficient for SnH_4, the value of $\sim 10^8\ s^{-1}$ was taken from Fig. 5 of Raynold[21] as guidance, specifically, the low temperature hydrogen adsorption onto molybdenum. Since hydrogen can not only physically adsorb but chemically bond to Sn as well, there will be a higher barrier to desorption. Thus, $K_0(SnH_4)$ was chosen to be an order of magnitude less than the molybdenum system,

$$\theta = \frac{K_{ads} n_{H(radical)}}{K_{ads} n_{H(radical)} + K_{des(H_2)} + K_{des}(SnH_4) + Y_i K_i n_i}, \tag{4}$$

$$\Gamma_{(SnH_4)} = (K_{des}(SnH_4) + Y_i K_i n_i)\theta n'. \tag{5}$$

$K_i = \sqrt{eT_e/m_i}/n'$ is the rate coefficient of ions incident on the surface, $Y_i \approx 0.009$[16] is the yield of SnH_4 desorbed per ion/radical, and $n' \approx 4.4{*}10^{19}/m^2$ is the surface area density. Total flux leaving the surface consists of SnH_4 given by Eq. (5).

TABLE I. Temperature effect in the etch rate process when pressure, power, and flowrate are constant. Added as the fourth reference point is the value of Ugur *et al.* (Ref. 12) when ions are not present.

Sample temperature (C)	No. of H per Sn removed ($m^2 s^{-1}$)	Θ	Experimental etch rate (nm/min)	Model etch rate (nm/min)
5 ± 1.5	417 ± 69	0.82 ± 0.07	110 ± 12.8	124 ± 16.6
40 ± 1.5	532 ± 88	0.48 ± 0.04	86 ± 8.5	85 ± 11.5
53 ± 1.5	675 ± 112	0.34 ± 0.03	68 ± 7.5	70 ± 9.3
Comparison case when no ions are present				
25[10]	90000[10]	0.64 ± 0.006	0.4 ± 0.05	0.47 ± 0.05

Published under license by AVS.

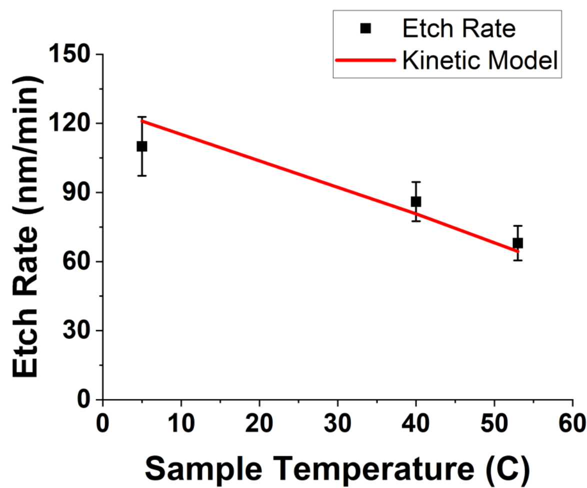

FIG. 10. Agreement of the etch rate with respect to the sample temperature with Gerlach-Meyer and Lieberman's kinetic etch model based on Eq. (7).

$n_{H(radical)} = 4.03{*}10^{19}/m^3$ is hydrogen radical density and n_i is ion density. The dominant term in Eq. (6) is $K_{des}(H_2)$, which is six orders of magnitude higher than $K_{des}(SnH_4)$ and much higher than $Y_i K_i n_i$ as well; thus, it can be rewritten as in Eq. (7). Knowing tin etch rates with and without ions, see Table I, helps determine pre-exponential factors for desorption rate equations. Temperature dependence results agree with Eq. (6) such that with the increase in temperature, $\kappa_{ads}(T)$ and $s(T)$ decrease, which consequently reduces adsorbed reactant density on the surface. Additionally, Zhang and Kushner,[22] Schaepkens *et al.*,[23] Gates *et al.*,[24] and Butterbaugh[25] show that with the increase in temperature, the etch rates decreases and the desorption rate increases (Fig. 10),

$$\text{Etch rate} = \frac{n'}{N_{sn}} \frac{K_{ads} n_{H(radical)} (K_{des}(SnH_4) + Y_i K_i n_i)}{K_{des}(H_2) + K_{des}(SnH_4) + Y_i K_i n_i + K_{ads} n_{H(radical)}}, \tag{6}$$

$$\text{Etch rate} \approx \frac{n'}{N_{sn}} \frac{K_{ads} n_{H(radical)} (K_{des}(SnH_4) + Y_i K_i n_i)}{K_{des}(H_2) + K_{ads} n_{H(radical)}}. \tag{7}$$

IV. SUMMARY AND CONCLUSIONS

This study shows the experimental results of tin etch rates by a surface wave plasma source. The Illinois NXE:3100 source was used to simulate the *in situ* operation of the linear SWP source on actual source conditions used in industry. We have determined the key parameters and mechanisms at work in etching Sn. Producing radicals and plasma at the location where cleaning is desired is the most important and efficient way to clean surfaces. High-rate Sn etching is achieved under realistic geometry and flow conditions that surpass the source contamination rate by a least of a factor of two. SWP is a very promising technology with industrial applications which can enhance the development of a lithographic tool in the semiconductor world. The next step is to scale the SWP power up, increasing the radial extent of the plasma, and better characterize this high powered SWP with etch rates, radical, and ion density measurements. Different antenna structures for the launcher might also increase areal plasma coverage over the collector. Experiments are underway at Illinois, which may make contribution to extending source lifetime.

ACKNOWLEDGMENTS

The authors are grateful for funding and support from ASML San Diego. Surface wave plasma equipment and consultations were provided by Starfire Industries. Parts of this research were carried out in the Frederick Seitz Materials Research Laboratory Central Facilities, University of Illinois, which is partially supported by the U.S. Department of Energy under Grant Nos. DEFG02-07ER46453 and DEFG02-07ER46471.

REFERENCES

[1]E. Hendrickx *et al.*, J. Photopolym. Sci. Technol. **26**, 587 (2013).
[2]J. A. Folta *et al.*, Proc. SPIE **3676**, 702 (1999).
[3]C. Eaborn, J. Organomet. Chem. **35**, C52 (1972).
[4]G. A. Panici, D. Qerimi, D. N. Ruzic, N. M. Felix, and K. A. Goldberg, Proc. SPIE **10143**, 101432I (2017).
[5]D. T. Elg, J. R. Sporre, G. A. Panici, S. N. Srivastava, and D. N. Ruzic, J. Vac. Sci. Technol. A **34**, 021305 (2016).
[6]D. N. Ruzic, "Scalable multi-role surface-wave plasma generator," U.S. patent 2014/0315347 A1 (23 October 2014).
[7]I. V. Fomenkov, A. A. Schafgans, D. C. Brandt, A. Ershov, Y. Tao, G. O. Vaschenko, and B. La Fontaine, in *EUV Lithography*, 2nd ed., edited by V. Bakshi (SPIE, Bellingham, WA, 2018).
[8]M. Mozetič, M. Kveder, M. Drobnič, A. Paulin, and A. Zalar, Vacuum **45**, 1095 (1994).
[9]D. Qerimi, "Radical probe system for *in situ* measurements of radical densities of hydrogen, oxygen and nitrogen," thesis (University of Illinois at Urbana-Champaign, 2019).
[10]M. Mozetic, A. Vesel, A. Drenik, I. Poberaj, and D. Babic, J. Nucl. Mater. **363–365**, 1457 (2007).
[11]D. Ugur, A. J. Storm, R. Verberk, J. C. Brouwer, and W. G. Sloof, Appl. Surf. Sci. **288**, 673 (2014).
[12]D. Ugur, A. J. Storm, R. Verberk, J. C. Brouwer, and W. G. Sloof, Chem. Phys. Lett. **552**, 122 (2012).
[13]O. V. Braginsky *et al.*, J. Appl. Phys. **111**, 093304 (2012).
[14]D. T. Elg, G. A. Panici, S. Liu, G. Girolami, S. N. Srivastava, and D. N. Ruzic, Plasma Chem. Plasma Process. **38**, 917 (2018).
[15]R. A. Rossen and H. H. Sawin, Appl. Phys. Lett. **45**, 860 (1984).
[16]M. A. Lieberman and A. J. Lichtenberg, *Principles of Plasma Discharges and Materials Processing Lieberman/Plasma 2e* (John Wiley & Sons, Inc., Hoboken, NJ, 2005).
[17]U. Gerlach-Meyer, Surf. Sci. **103**, 524 (1981).
[18]H. Meiling, V. Banine, N. Harned, B. Blum, P. Kuerz, and H. Meijer, Proc. SPIE **5751**, 90 (2005).
[19]H. Schade, Z. E. Smith, J. H. Thomas, and A. Catalano, Thin Solid Films **117**, 149 (1984).
[20]F. Martin, X. Feaugas, A. Oudriss, D. Tanguy, L. Briottet, and J. Kittel, *Mechanics—Microstructure—Corrosion Coupling* (Elsevier, London, 2019), pp. 171–197.
[21]T. W. Raynolds, "Adsorption-desorption behavior of homogeneous and heterogeneous metal surfaces," Technical Note NASA-TN-D-4789 (NASA, 1968).

Published under license by AVS.

[22]D. Zhang and M. J. Kushner, J. Appl. Phys. **87**, 1060 (2000).
[23]M. Schaepkens, R. C. M. Bosch, T. E. F. M. Standaert, G. S. Oehrlein, and J. M. Cook, J. Vac. Sci. Technol. A **16**, 2099 (1998).
[24]S. M. Gates, C. M. Greenlief, S. K. Kulkarni, and H. H. Sawin, J. Vac. Sci. Technol. A **8**, 2965 (1990).
[25]J. W. Butterbaugh, J. Vac. Sci. Technol. B **9**, 1461 (1991).

Published under license by AVS.